

Article

A Density Functional Study on Ethylene Trimerization and Tetramerization Using Real Sasol Cr-PNP Catalysts

Minserk Cheong * and Ajeet Singh 

Department of Chemistry, Research Institute for Basic Sciences, Kyung Hee University, Seoul 02447, Republic of Korea

* Correspondence: mcheong@khu.ac.kr

Abstract: To gain molecular-level insight into the intricate features of the catalytic behavior of chromium–diphosphine complexes regarding ethylene tri- and tetramerizations, we performed density functional theory (DFT) calculations. The selective formation of 1-hexene and 1-octene by the tri- and tetramerizations of ethylene are generally accepted to follow the metallacycle mechanism. To explore the mechanism of ethylene tri- and tetramerizations, we used a real Sasol chromium complex with a nitrogen-bridged diphosphine ligand with *ortho*- and *para*-methoxyaryl substituents. We explore the trimerization mechanism for ethylene first and, later on for comparison, we extend the potential energy surfaces (PES) for the tetramerization of ethylene with both catalysts. The calculated results reveal that the formation of 1-hexene and 1-octene with the *ortho*-methoxyaryl and *para*-methoxyaryl Cr-PNP catalysts have nearly similar potential energy surfaces (PES). From the calculated results important insights are gained into the tri- and tetramerizations. The tetramerization of ethylene with the *para*-methoxyaryl Cr-PNP catalyst lowers the barrier height by ~2.6 kcal/mol compared to that of ethylene with the *ortho*-methoxyaryl Cr-PNP catalyst. The selectivity toward trimerization or tetramerization comes from whether the energy barrier for ethylene insertion to metallacycloheptane is higher than β -hydride transfer to make 1-hexene. The metallacycle mechanism with Cr (I)–Cr (III) intermediates is found to be the most favored, with the oxidative coupling of the two coordinated ethylenes to form chromacyclopentane being the rate-determining step.



Citation: Cheong, M.; Singh, A. A Density Functional Study on Ethylene Trimerization and Tetramerization Using Real Sasol Cr-PNP Catalysts. *Molecules* **2023**, *28*, 3101. <https://doi.org/10.3390/molecules28073101>

Academic Editors: Giuseppe Cirillo, Diego Muñoz-Torrero and Roman Dembinski

Received: 18 March 2023

Revised: 28 March 2023

Accepted: 28 March 2023

Published: 30 March 2023



Copyright: © 2023 by the authors. Licensee MDPI, Basel, Switzerland. This article is an open access article distributed under the terms and conditions of the Creative Commons Attribution (CC BY) license (<https://creativecommons.org/licenses/by/4.0/>).

1. Introduction

Linear α -olefins (LAOs) are valuable building blocks for a range of industrial and consumer products, including surfactants, comonomers, and synthetic lubricants [1–7]. At present, the bulk of LAOs is produced through metal-catalyzed ethylene oligomerization processes. The industrial use of linear α -olefins depends mainly on the chain length, with lower C₄–C₈ oligomers used as comonomers for ethylene polymerization. Several related processes are in use at present, with the most important being the production of high-density polyethylene (HDPE) and linear low-density polyethylene (LLDPE) [8].

Selective catalysts for the oligomerization of ethylene have been developed by Phillips [9]. Producing 1-hexene or 1-octene without any other by-products can have significant environmental benefits. These catalysts consist of a substituted pyrrole ligand, a chromium source, and an alkyl aluminum activator. These catalysts achieve the good selectivity of 1-hexene and have remained the state of the art for many years. Most research in the area has focused on minor modifications to these systems until very recently [10–13].

Since the early discovery of a selective trimerization catalyst by Manyik et al. of the Union Carbide Corporation, several catalyst systems based on chromium and titanium have been developed [14]. The production of 1-hexene by these catalysts was explained by the same author, who proposed for the first time the involvement of metallacycles as key intermediates (Figure 1, Path a). This mechanism was expanded by Briggs [15] (Figure 1,

Path b), who suggested the third ethylene molecule interacts with metallacyclopentane to yield metallacycloheptane instead of forming a dialkyl intermediate, as suggested by Manyik et al. Many experiments and density functional theory (DFT) studies have been performed to prove the metallacycle mechanism since then. Emrich et al. obtained the crystal structures of the intermediates and confirmed that the two metallacycles are involved in the mechanism. They also demonstrated that the metallacyclopentane is more stable than metallacycloheptane and that the latter decomposes with the liberation of 1-hexene [16]. Furthermore, Agapie et al. successfully distinguished the metallacycle mechanism for selective trimerization on a chromium-PNP catalyst from a Cossee-type mechanism [17,18] for non-selective ethylene oligomerization on a nickel-based catalyst through deuterium-labeling experiments [19,20]. Later, an NMR study by Arteaga-Müller et al. confirmed that metallacyclopentane and metallacycloheptane are important intermediates responsible for ethylene trimerization into 1-hexene [21].

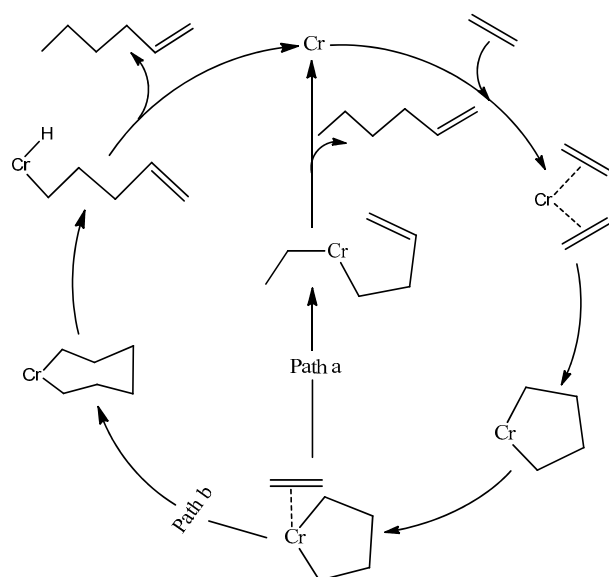


Figure 1. Proposed mechanism of ethylene trimerization.

Although extensive experimental and theoretical studies have been conducted, many important mechanistic details for trimerization remain unclear, although the metallacycle mechanism is widely accepted. The two proposed oxidation states of chromium are I/III or II/IV [22–26]. The variable oxidation states of organometallic complexes make computational calculations notoriously difficult, with SCF convergence problems and the computationally expensive nature of open shell calculations [27]. These phenomena are likely the reasons why theoretical studies based on Cr chemistry are less frequently studied than those based on other transition metals. Recent calculations emphasize the importance of spin state change during the reaction of transition metal compounds [28–31]. DFT studies by Budzelarr for a chromium indolate-AlR₂Cl catalyst and Britovsek et al. and Gong et al. for chromium-PNP catalysts suggest that chromium (I/III) has a reasonable possibility for ethylene trimerization compared to chromium (II/IV) [32–34]. Not only the DFT study but also many other experimental studies on the Cr-PNP system have been considered the active species of Cr to be in the oxidation state I/III during the catalytic cycle [20,35,36]. In this study, we start calculations with chromium (I) and perform the spin state change of chromium from I to III during the course of the reaction.

A plethora of catalyst systems, mostly based on chromium [14–16,37–48], although others including titanium [49–51], nickel [52], and tantalum [53] are also known, exhibit a surprisingly high selectivity for the trimerization of ethylene to form 1-hexene. The most prominent among these is the chromium PNP catalyst system discovered by Wass et al., which comprises Ar₂PN (Me) PAr₂ (Ar = *ortho*-methoxy-substituted aryl group). Upon

activation with methyl aluminoxane (MAO), the catalyst yielded highly selective 89.9 wt% 1-hexene with unprecedented productivity [40]. This figure of merit is about two orders of magnitude greater than previous systems under similar conditions. Furthermore, the experimental approach by Overett et al. to elucidate the role of methoxy substitution at the aromatic ring of the PNP ligand revealed that *ortho*-methoxy substitution plays a vital role in the catalytic performance for the selective trimerization of ethylene [54]. Changing the methoxy substitution from *ortho* to *meta* led to a drastic swing in chain-length distribution from predominantly 1-hexene to a significantly greater amount of 1-octene. This swing towards ethylene tetramerization was even more pronounced when the methoxy group was further moved to the *para* position [40]. The experimental mechanistic study provided evidence for metallacyclic mechanism as well as insights into the nature of the active site for such systems. However, there is a lack of common understanding regarding the high selectivity towards the trimerization of ethylene and the selectivity swing with substituent position with these (Cr-1 and Cr-2, with ligands in Figure 2) catalysts.

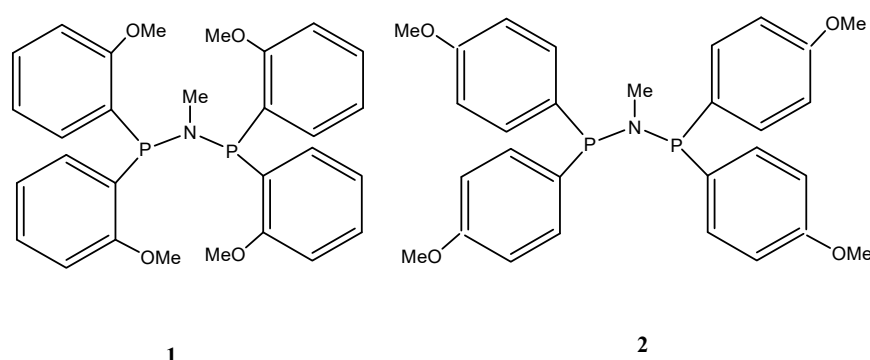


Figure 2. *Ortho*- and *para*-methoxyaryl PNP ligands.

Bis-ethylene *ortho*- and *para*-methoxyaryl Cr-PNP catalysts are our starting species, in which chromium has the oxidation state I (1R and 2R). After Cr (I) is oxidized to Cr (III) (1SC1 and 2SC1), a five-membered metallacycle is formed (1INT1 and 2INT1). However, since no 1-butene is experimentally observed, the reaction is believed to continue to obtain 1INT2 and 2INT2, in which a third ethylene molecule is coordinated. After the ethylene insertion (1INT3 and 2INT3), the reaction might proceed with a ring opening to finally produce 1-hexene. Alternatively, the reaction may proceed with the insertion of a new ethylene molecule to yield 1INT4 and 2INT4, which leads to 1-octene.

In the present theoretical study, we explore the tri- and tetramerization reactions of ethylene by applying density functional theory using *ortho*- and *para*-methoxyaryl Cr-PNP catalysts, to find a theoretical explanation for the observed experimental selectivity. To the best of our knowledge, no theoretical study with the real Sasol Cr-catalyzed mechanism for ethylene tri- and tetramerizations has been reported. In this DFT study, we use catalysts without any simplification to study the subtle steric effects more accurately, which are commonly lacking in previous theoretical studies [55], especially with Cr-PNP based catalysts.

2. Results and Discussion

2.1. Structure and Bonding Aspects of the *Ortho*-Methoxyaryl Cr-PNP Catalyst

The optimized geometries for the *ortho*-methoxyaryl Cr-PNP catalyst participating in the ethylene trimerization and tetramerization mechanisms are presented in Figure 3. The Cr (I) sextet species 1R is considered the first active complex in the tri- and tetramerization cycle for the *ortho*-methoxyaryl Cr-PNP catalyst. The optimized structure 1R has a tetrahedral geometry with Cr-P distances of 2.631 and 2.733 Å. Initially, both ethylene molecules are weakly coordinated to Cr (I) via π -bonding interactions. The relatively weak nature

of the π -bonding is reflected in the relatively shorter C-C bonding distance of 1.353 and 1.357 Å, which is 0.022–0.026 Å longer than the calculated C=C distance in free ethylene.

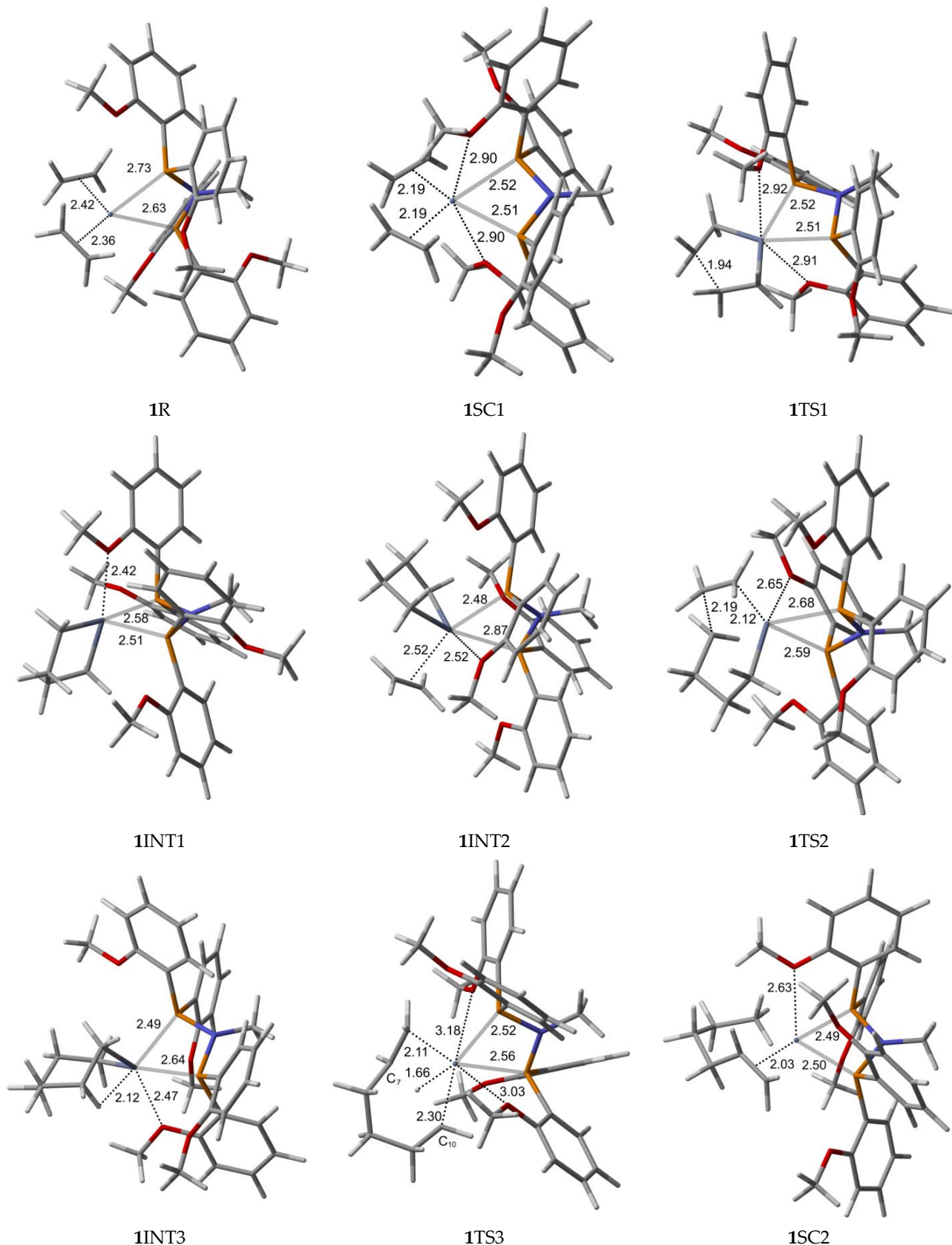


Figure 3. *Cont.*

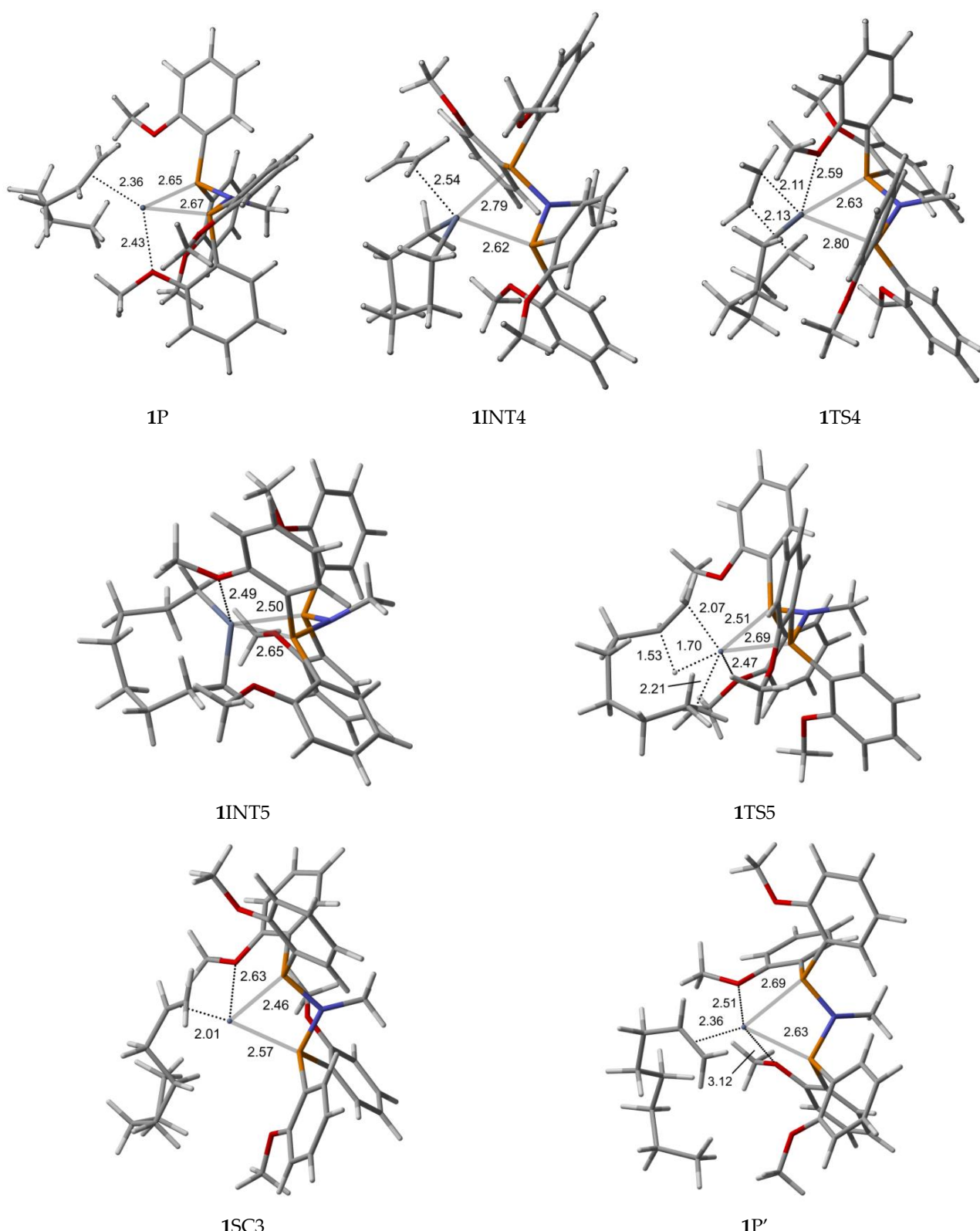


Figure 3. B3LYP/6-31G^{*}/LanL2DZ optimized geometries (Supplementary Material) with important distances (\AA) for ethylene trimerization and tetramerization using the *ortho*-methoxyaryl Cr-PNP catalyst. (Gray: carbon; red: oxygen; white: hydrogen; orange: phosphorus; blue: nitrogen; dark gray: Cr).

Furthermore, the Cr-C distances for both ethylene fragments are 2.363 and 2.418 Å, which indicates that both ethylenes are coordinated with nearly equal strength. During the catalytic cycle, it is known that the spin state of Cr changes [31,56], implying that at least one other stable structure exists between the reactants and the transition state. Therefore, we located the possible spin crossover quartet **1SC1** complex between the reactant and first transition state **1TS1**. The calculated structure of complex **1SC1** has an octahedral geometry with two of the four methoxy groups approaching from the apical positions with Cr-O distances of 2.897 Å and 2.904 Å and the two ethylene fragments are more tightly coordinated to Cr (I) with distances of 2.191 Å compared to **1R**. Two ethylene molecules moved to the same plane as the PNP ligand, making room for these two methoxy groups to coordinate with the chromium metal. This hemilabile behavior of the methoxy groups upon the coordination to Cr is vital in the catalytic activity and selectivity. The formation of the five-membered metallacyclic Cr (III) species **1INT1** is afforded by the oxidative addition of the two ethylene fragments via the transition structure **1TS1**. In octahedral **1TS1** with the apical Cr-O distances of 2.907 Å and 2.917 Å, the coupling C-C distance of the ethylenes decreases from 2.614 Å in **1SC1** to 1.942 Å. The five-membered metallacycle product **1INT1** has a C-C coupling distance of 1.536 Å, which agrees with the expected distance for the C-C single bond. Because of the position of the metallacyclic ring, the structure is trigonal bipyramidal. This coordination behavior of the ortho-methoxy group to Cr (III) has a profound steric effect and an electronic effect throughout the catalytic cycle. In order for ethylene trimerization to proceed, the incorporation of a third ethylene molecule is necessary. The interaction of ethylene with the trigonal bipyramidal five-membered metallacycle **1INT1** affords octahedral **1INT2**, in which the ethylene fragment is weakly coordinated via a long-range π -interaction. This is evident from the elongated Cr-C distances of 2.522 Å for Cr-ethylene in **1INT2**, as well as the relatively short C=C distance of 1.345 Å for the coordinated ethylene fragment (Figure 3). Metallacycle growth from **1INT2** to **1INT3** via **1TS2** yields the seven-membered metallacycle with β -agostic hydrogen. In order for the liberation of 1-hexene to proceed from the seven-membered metallacycles, **1INT3**, the reductive migration of this β -agostic hydrogen needs to take place. The Cr-mediated hydrogen migration from C7 in **1TS3** to C10 yields 1-hexene, coordinated to the resulting quartet **1SC2** with a Cr (I) oxidation state. In **1TS3**, the methoxy group, which previously coordinated to Cr, moves away from Cr, possibly because of the sterically crowded environment of the transition state. However, the other methoxy group moves in to compensate for the electronic requirement of the catalyst. Then, spin crossover from seesaw quartet **1SC2** provides the more stable tetrahedral sextet **1P**, both with coordinated methoxy groups.

To investigate the possibility of tetramerization with this catalyst, we extended the PES for the next insertion of ethylene. The coordination of the fourth ethylene to **1INT3** forms intermediate **1INT4**. In **1INT4**, the distance of C1 and C6 with Cr is 2.043 and 2.028 Å, respectively, while the newly coordinated ethylene is 2.536 Å away, indicating a weak Cr-ethylene interaction. The most important change in the coordination sphere is the absence of the methoxy group. The seven-membered metallacycle and ethylene are sterically crowded enough to move the methoxy groups out of the coordination sphere. The formation of the nine-membered metallacycle Cr(III) species **1INT5** is achieved via the transition structure **1TS4**. In **1TS4**, the coupling distance of C-C decreases from 3.160 Å to 2.127 Å. Additionally, the coordination of the methoxy group occurs since the ethylene moiety moves closer to metallacycle to create space. The nine-membered metallacycle product **1INT5** has a C-C coupling distance of 1.544 Å, which is in agreement with the expected distance for the C-C single bonds. Then, the migration of the β -agostic hydrogen yields seesaw **1SC3** via **1TS5**, and the spin crossover produces the more stable trigonal bipyramidal sextet **1P'**.

2.2. Structure and Bonding Aspects of the Para-Methoxyaryl Cr-PNP Catalyst

To explore the catalytic behavior of the para-methoxyaryl Cr-PNP catalyst, we performed calculations and located the stationary structures along the PES. All the optimized structures for trimerization and tetramerization are presented in Figure 4. Compared to the ortho-methoxyaryl Cr-PNP catalyst, there is no coordination of the methoxy group to chromium in the para-methoxyaryl Cr-PNP catalyst. This leads to a significant difference in the structures and energetics of the system.

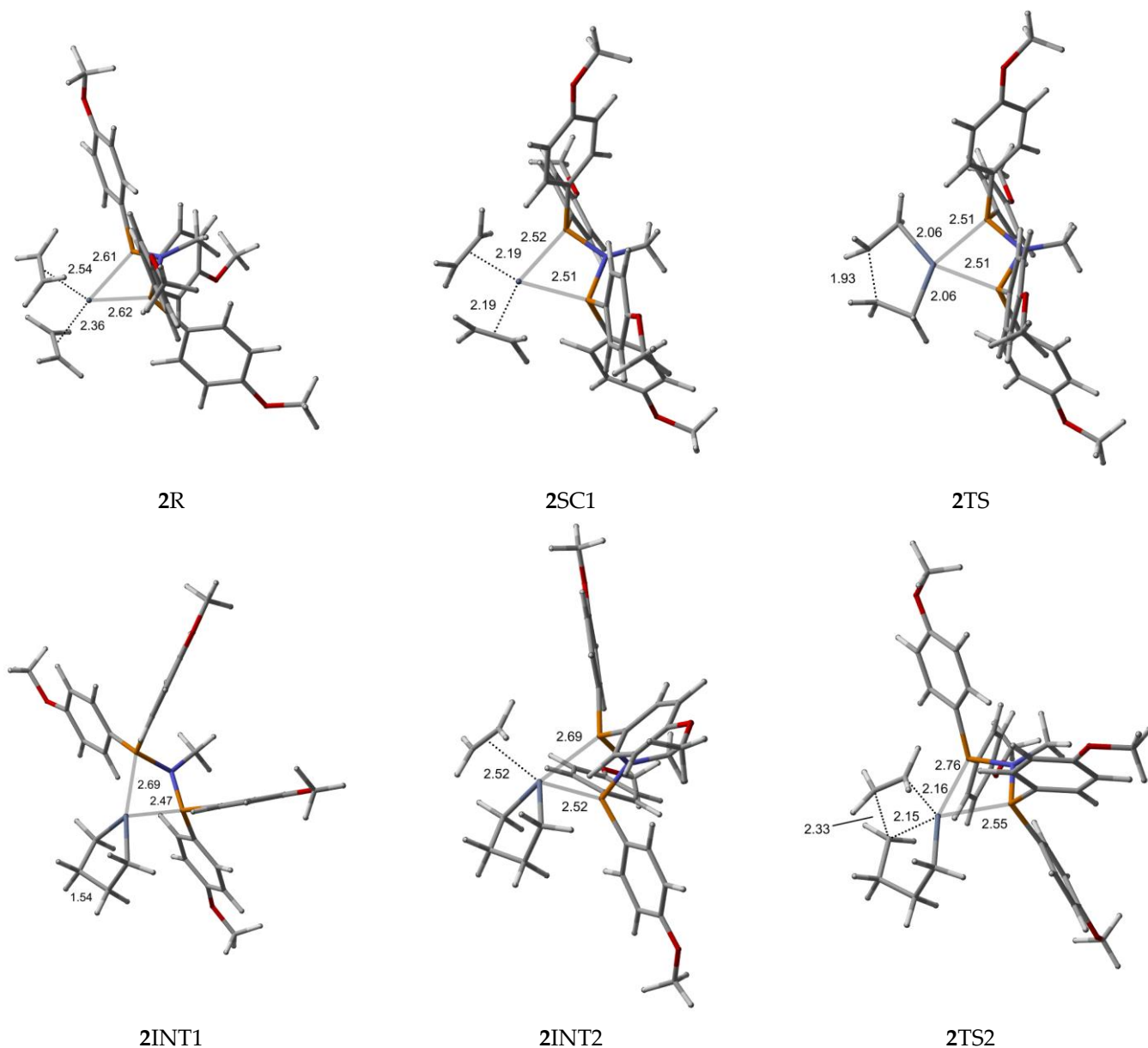


Figure 4. Cont.

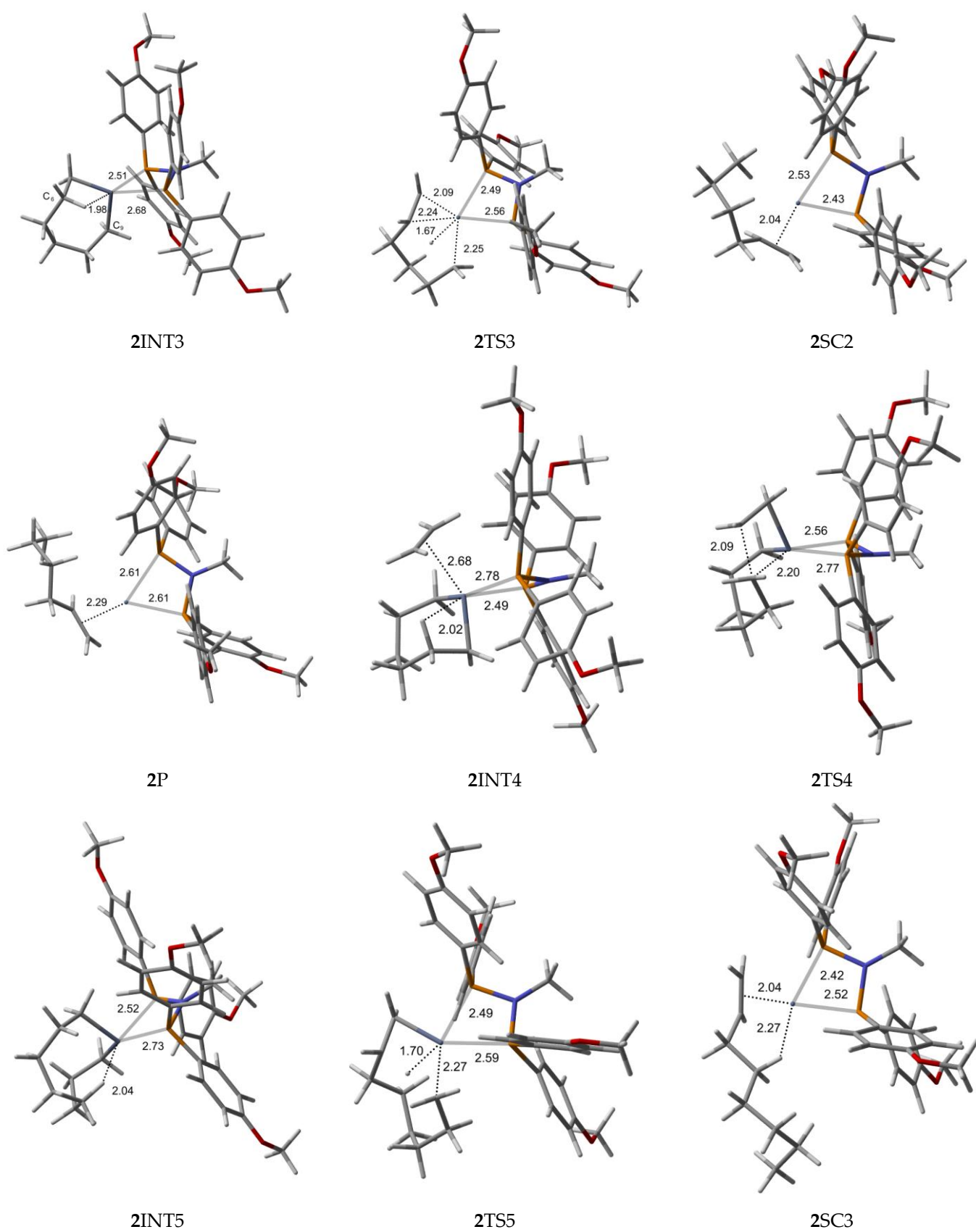


Figure 4. Cont.

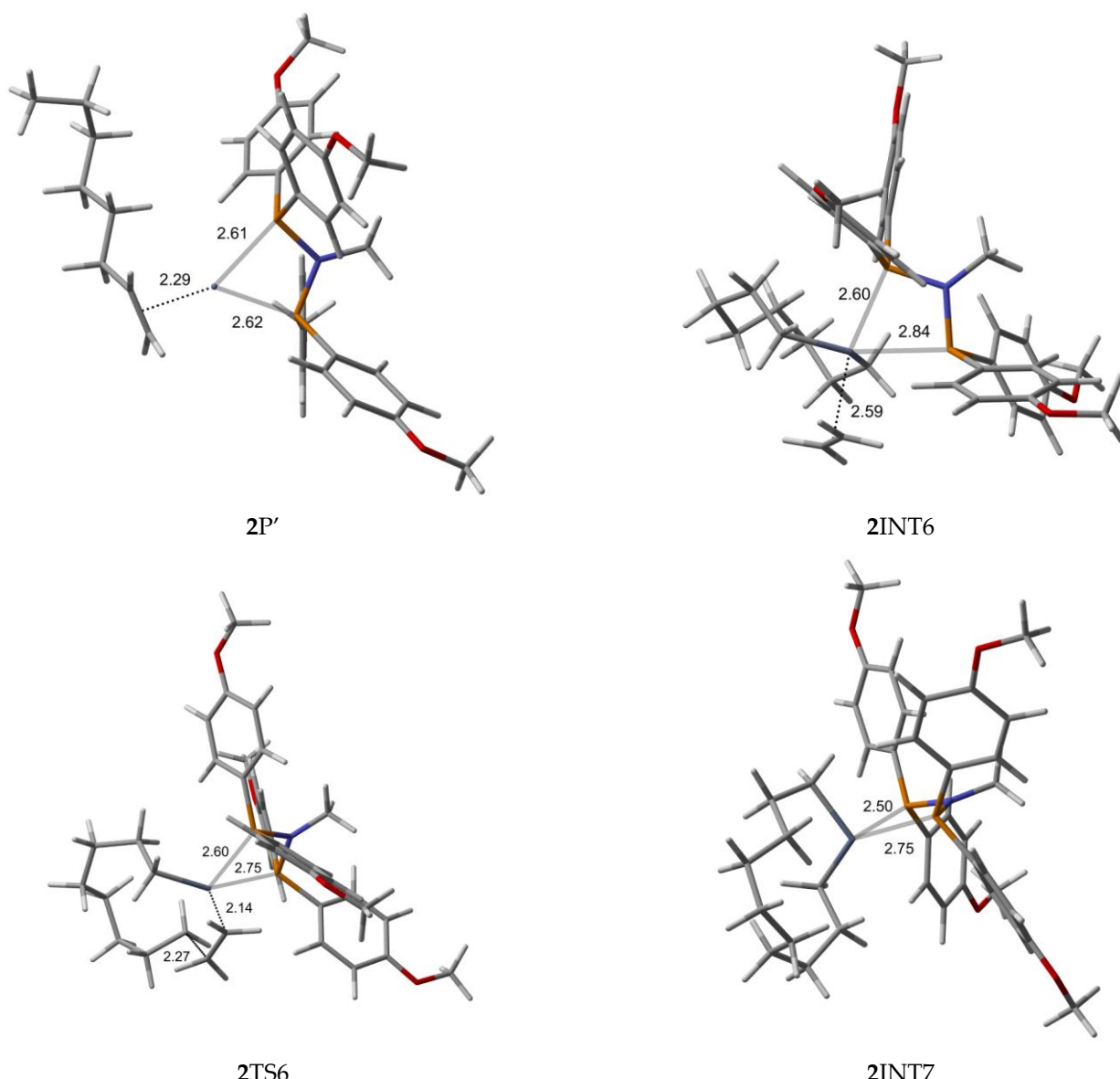


Figure 4. B3LYP/6-31G*/LanL2DZ optimized geometries (Supplementary Material) with important distances (\AA) for ethylene trimerization and tetramerization using the *para*-methoxyaryl Cr-PNP catalyst. (Gray: carbon; red: oxygen; white: hydrogen; orange: phosphorus; blue: nitrogen; dark gray: Cr).

The Cr (I) sextet species **2R** is considered the first active complex in the tri- and tetramerization cycle for the *para*-methoxyaryl Cr-PNP catalyst. The optimized structure **2R** has a tetrahedral geometry with Cr-P distances of 2.613 and 2.622 \AA . Initially, both ethylene molecules are weakly coordinated to Cr(I) via π -bonding interactions. The relatively weaker nature of the π -bonding is reflected in the relatively shorter C-C bonding distances of 1.348 and 1.359 \AA , which are 0.017–0.028 \AA longer than the calculated C=C distance in free ethylene. Furthermore, the Cr-C distances for both ethylene fragments are 2.355 and 2.542 \AA , indicating that both ethylene fragments are coordinated with nearly equal strength. As in the *ortho*-methoxyaryl Cr-PNP catalyst, we located the possible spin crossover quartet **2SC1** complex between the reactant and first transition state **2TS1**. The calculated structure of complex **2SC1** has a square-planar geometry, and the two ethylene fragments are more tightly coordinated to Cr (I) with distances of 2.19 \AA compared to **2R**. The formation of the five-membered metallacycle Cr (III) species **2INT1** is afforded by the oxidative addition

of the two ethylene fragments via the transition structure **2TS1**. In square-planar **2TS1**, the C-C coupling distance of the ethylenes decreases from 2.611 Å in **2SC1** to 1.930 Å. The five-membered metallacycle product **2INT1** has C-C coupling distances of 1.539 Å, which is in agreement with the expected distance for C-C single bonds. In order for ethylene trimerization to proceed, the incorporation of a third ethylene molecule is necessary. The interaction of ethylene with the square-planar five-membered metallacycle **2INT1** affords square-pyramidal **2INT2**, in which the ethylene fragment is weakly coordinated via a long-range π -interaction. This is evident from the elongated Cr-C distances of 2.521 Å for Cr-ethylene in **2INT2**, as well as the relatively short C=C distance of 1.347 Å for the coordinated ethylene fragment (Figure 4). Metallacycle growth from **2INT2** via **2TS2** to **2INT3** yields the seven-membered metallacycle. To proceed with the liberation of 1-hexene from the seven-membered metallacycle (**2INT3**), reductive hydrogen migration from C6 to C9 is required. The migration of the β -agostic hydrogen of C6 in **2INT3** to C9 leads to the formation of an agostic intermediate structure via the transition structure **2TS3**. The Cr-mediated hydrogen migration from C6 in **2TS3** to C9 yields 1-hexene, coordinated to the resulting T-shaped quartet **2SC2** with Cr (I) oxidation state. Then, spin crossover occurs and yields a more stable trigonal planar sextet **2P**.

To explore the possibility of tetramerization with this catalyst, we extended the PES for the next insertion of ethylene. The coordination of the fourth ethylene to **2INT3** forms an intermediate **2INT4**. In **2INT4**, the distance between Cr and the newly coordinated ethylene is 2.678 Å, indicating a weak Cr-ethylene interaction. The formation of the nine-membered metallacycle Cr (III) species **2INT5** is achieved via the transition structure **2TS4**. In **2TS4**, the C-C coupling distance decreases from 3.384 Å to 2.086 Å. The nine-membered metallacycle products **2INT5** have C-C coupling distances of 1.545 Å, which agrees with the expected distance for a C-C single bond. Then, the migration of the β -agostic hydrogen yields **2SC3** via **2TS5**, and the spin crossover produces a more stable sextet **2P'**.

Furthermore, we explored the possibility of pentamerization for the reasons explained in the subsequent section. The coordination of the fourth ethylene to **2INT5** forms an intermediate **2INT6**. The formation of the eleven-membered metallacycle Cr(III) species **2INT7** is achieved via the transition structure **2TS6**.

2.3. Energetic Aspects of the Cr-PNP Catalyst

The structures **1R** and **2R** were chosen as a reference structure, and the energies of the following intermediates, transition states, and products are related to **1R** and **2R**, corrected with the right number of ethylene molecules. In Figures 5 and 6, free energy profiles (in kcal/mol) are plotted for the stationary points along the reaction pathway. The energies for the optimized structures were corrected by triple-zeta single-point calculations at the 6-311++G(d,p) level of theory with Grimme's D3 empirical dispersion corrections, including Becke-Johnson damping. Additionally, corrections for reactions in the liquid phase were conducted using the SMD polarizable continuum solvent model augmented with parameters for toluene. The conversions of the *bis*-ethylene complexes **1R** and **2R** to the corresponding metallacyclopentanes, **1INT1** and **2INT1**, are endothermic reactions by 6.8 kcal/mol and 10.2 kcal/mol, respectively. The formal oxidative coupling of two ethylene molecules occur via the transition states **1TS1** and **2TS1** with activation energy barriers of 16.3 kcal/mol and 20.0 kcal/mol, respectively. The extra stabilization of 3.4–3.7 kcal/mol of the *ortho*-methoxyaryl Cr-PNP catalyst compared to that of the *para*-methoxyaryl Cr-PNP catalyst is due to the coordination of the *ortho*-methoxy group to the chromium metal ion.

This effect persists until the catalytic cycle reaches **1INT4** and **2INT4**, at which point ethylene coordinates to metallacycloheptane, making the coordination sphere crowded enough to prevent the coordination of the *ortho*-methoxy group. This raises the energy of **1INT4** compared to **2INT4**. The experimental evidence indicates that, with the Cr-PNP catalytic system, the rate-determining step is the oxidative coupling of the first two ethylene molecules to form the metallacyclopentane intermediate [57]. Our calculated result for both the *ortho*- and *para*-methoxyaryl Cr-PNP catalysts reaches a similar conclusion, with the

activation energies of 16.3 and 20.0 kcal/mol, respectively, which are in good agreement with the experimental results.

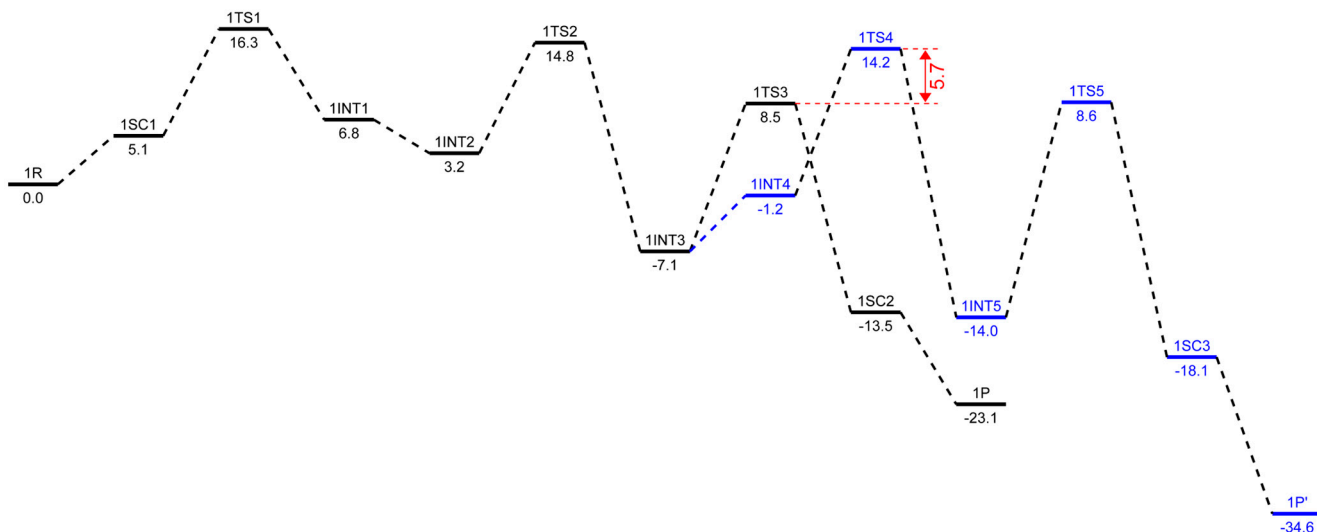


Figure 5. Corrected free energy profiles (in kcal/mol) at the level of B3LYP/6-311++G(d,p) with GD3BJ for ethylene trimerization in black and tetramerization in blue, using the *ortho*-methoxyaryl Cr-PNP catalyst. The SMD polarizable continuum solvent model was used for solvent effect correction.

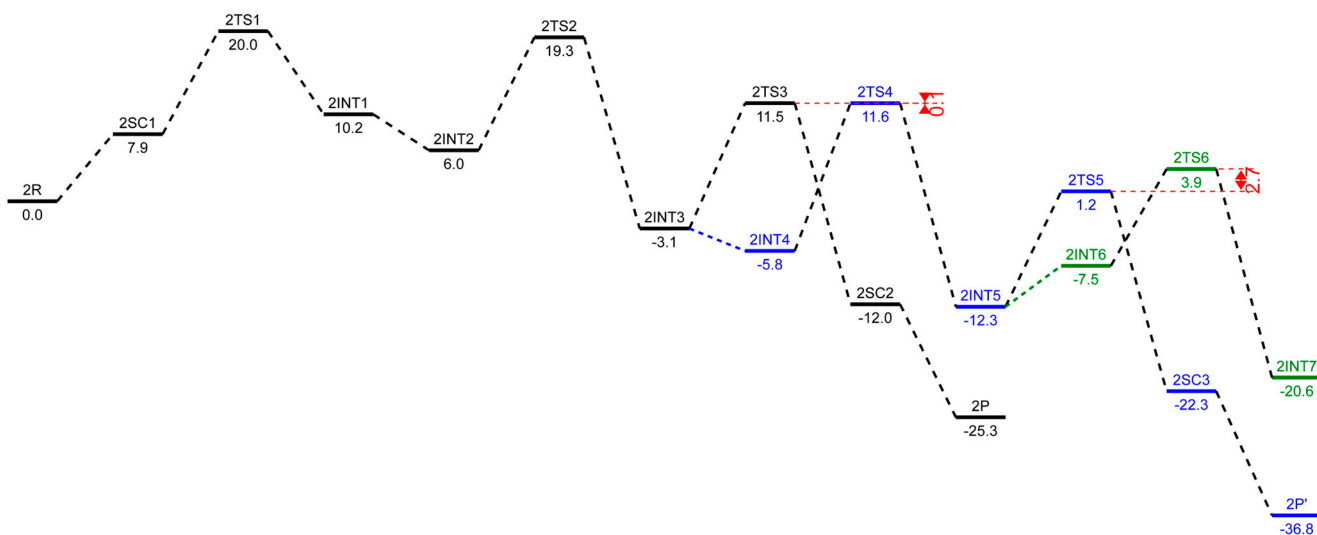


Figure 6. Corrected free energy profiles (in kcal/mol) at the level of B3LYP/6-311++G(d,p) with GD3BJ for ethylene trimerization in black, tetramerization in blue, and pentamerization in green using the *para*-methoxyaryl Cr-PNP catalyst. The SMD polarizable continuum solvent model was used for solvent effect correction.

There is a fair chance that the chromacyclopentane undergoes a ring-opening reaction, but no experimental evidence has been found for the formation of 1-butene with these catalysts, so we did not attempt to locate the transition state for ring opening with a five-membered metallacycle ring. The third ethylene molecule was added to the intermediate **1INT1** or **2INT1** to form **1INT2** or **2INT2**, and both processes were downhill by 3.6 and 4.2 kcal/mol, respectively. The subsequent conversion of **1INT2** or **2INT2** to the intermediate **1INT3** or **2INT3** occurs via the insertion of ethylene into the Cr-C bond through the transition state **1TS2** or **2TS2**, respectively. However, both intermediates stabilize at nearly the same energetic values and are also exothermic in nature with -10.3 and -9.1 kcal/mol, respectively. The activation barriers for both **1INT2-1INT3** and **2INT2-2INT3** are 14.8 and

19.3 kcal/mol, respectively. The conversion of the intermediate **1INT3** or **2INT3** to produce 1-hexene occurs via an agnostic-assisted hydride transfer [58,59]. The transition states (**1TS3** and **2TS3**) associated with these conversions have activation energy barriers of 8.5 and 11.5 kcal/mol, respectively. The products **1SC2** and **2SC2** are the most stable intermediates in their respective catalytic cycle, with relative energies of −13.5 and −12.0 kcal/mol, respectively. We also located the spin crossover complexes with Cr(I) (**1P** and **2P**), which are very low in energy, with −23.1 and −25.3 kcal/mol, respectively, compared to the Cr (III) oxidation state intermediates (**1SC2** and **2SC2**).

The calculated results of the trimerization with the *ortho*- and *para*-methoxyaryl Cr-PNP catalysts indicate that both tend to form 1-hexene, which was also observed experimentally, even though with the *para*-methoxyaryl Cr-PNP catalyst, the percentage of trimerization product is low. To address the question of why there is a selectivity change or shift from trimerization to tetramerization with the shifting of the −OMe substituent on the ligand backbone, we extended the PES and located the stationary points with the fourth molecule of ethylene. The subsequent conversion of **1INT3** or **2INT3** to the intermediate **1INT4** or **2INT4** occurs via the coordination of another ethylene molecule. There is a great difference in energy between the *ortho*-methoxyaryl Cr-PNP catalyst and the *para*-methoxyaryl Cr-PNP catalyst. In the case of the *para*-methoxyaryl Cr-PNP catalyst, it is an exothermic reaction by 2.7 kcal/mol, as in the conversion of **2INT1** to **2INT2**. However, in the case of the *ortho*-methoxyaryl Cr-PNP catalyst, the reaction becomes endothermic by 5.9 kcal/mol. The reason for the considerable difference comes from the absence of the coordination of the *ortho*-methoxy group in moving from **1INT3** to **1INT4** because of steric crowdedness in the coordination sphere. This steric effect also affects the insertion of ethylene into the Cr-C bond via the transition state **1TS4** (Figure 5). The activation barriers of both **1INT4**–**1INT5** and **2INT4**–**2INT5** are 14.2 and 11.6 kcal/mol, respectively. This shows that the *ortho*-methoxyaryl Cr-PNP catalyst suffers more steric hindrance than the *para*-methoxyaryl Cr-PNP catalyst, as expected. Energy barriers for the metallacycle expansion of ring from seven- to nine-membered (chromium-cyclononane) are very high. Such an exceptionally high energy can be explained by means of steric effects and the instability of the nine-membered ring. The calculated results indicate that the formation of 1-hexene is kinetically preferred with both catalysts, while the formation of 1-octene with these catalysts seems to be unfavored, even though with the *para*-methoxyaryl Cr-PNP catalyst, the energy barrier for tetramerization is lowered by ~2.7 kcal/mol than that of *ortho*-methoxyaryl Cr-PNP catalyst, making it almost the same as the energy barrier for trimerization. Therefore, the key to selectivity toward trimerization or tetramerization depends on the difference in transition state energy between ring expansion and β-hydride transfer. In the case of the *ortho*-methoxyaryl Cr-PNP catalyst, the β-hydride transfer is lower in energy than ring expansion by 5.7 kcal/mol (shown in red in Figure 5). This energy difference is large enough to prevent ring expansion, so experimentally, 82~91% selectivity toward 1-hexene is observed [20]. In the case of the *para*-methoxyaryl Cr-PNP catalyst, the energy difference is almost zero (shown in red in Figure 6). So, experimentally, only 38–50% selectivity toward 1-octene is observed [20], since both trimerization and tetramerization can occur. These calculation results surprisingly coincide with the experimental results very well. This can only happen with extensive conformational search and accurate energy calculation with dispersion and damping. The conversion of intermediate **1INT5** or **2INT5** to produce 1-octene occurs via agnostic-assisted hydride transfer. Both transition states (**1TS5** and **2TS5**) associated with these conversions have activation energy barriers of 8.6 and 1.2 kcal/mol, respectively. The products **1SC3** and **2SC3** are the most stable intermediates in their respective catalytic cycles, with relative energies of −18.1 and −22.3 kcal/mol, respectively. We also located the spin crossover complexes with Cr (I) (**1P'** and **2P'**), which are very low in energy, with −34.6 and −36.8 kcal/mol, respectively.

In case of the *para*-methoxyaryl Cr-PNP catalyst, both trimerization and tetramerization can occur. So, we have to investigate whether ring expansion can occur further. The conversion of **2INT5** to the intermediate **2INT6** occurs via the coordination of another

ethylene. The reaction is endothermic by 4.8 kcal/mol, which is different from the same ethylene coordination from 2INT3 to 2INT4. The reason for the difference comes from the steric crowdedness in the coordination sphere with the larger metallacycle. This steric effect also affects the insertion of ethylene into the Cr-C bond via the transition state 2TS6 (Figure 6) with the activation barriers of 3.9 kcal/mol. The energy barrier for the metallacycle ring expansion from nine to eleven is higher than that of the β -hydride transfer to produce 1-octene by 2.7 kcal/mol (shown in red in Figure 6). Therefore, we can expect that the further expansion of metallacycle to an 11-membered ring is unfavorable, as shown in the experimental results.

The experimental results show that changing from *ortho*-methoxy to *para*-methoxy in the catalyst backbone causes a shift in product distribution from 1-hexene only to a mixture of 1-octene and 1-hexene. In this study, we attempted to explain this mechanism using DFT calculations and found out that, with the *ortho*-methoxyaryl PNP ligand, the methoxy group is in close proximity to the chromium metal for coordination and plays a major role in the catalytic cycle, resulting in the production of only 1-hexene. Conversely, with the *para*-methoxyaryl PNP ligand, this coordination does not occur, and the product distribution is determined solely by steric hindrance from the phenyl group, resulting in an almost 50:50 ratio of 1-hexene to 1-octene.

3. Computational Methods

Geometries were fully optimized using the non-local B3LYP method, which is a combination of Becke's three-parameter hybrid exchange functional and the correlation functional of Lee, Yang, and Parr [60–62], without any symmetry constraints. The LANL2DZ (Los Alamos National Laboratory second double-zeta) basis set was used for Cr atoms, while the 6-31G* basis set was used for C, H, N, O and P atoms [63,64], with the GAUSSIAN 16 program package [65]. Harmonic force constants were computed for the optimized geometries to characterize the stationary points as minima. The number of imaginary frequencies (Imag) at the same level of theory, i.e., energy minimum structures without imaginary frequencies (NImag = 0) and transition states with only one imaginary frequency (NImag = 1), confirmed whether the optimized structures are transition states or true minima on the potential energy surfaces. The magnitude of the imaginary frequency and the corresponding eigenvectors were analyzed for all transition states to verify the involvement of the required atoms.

Exhaustive conformational searching was performed for all ground-state and transition state structures, but only the lowest-energy structures are reported. The energies of reactants, transition states, and products were corrected by triple-zeta single-point calculation at the 6-311++G(d,p) level of theory. Dispersion corrections were included using the D3 empirical correction from Grimme [66], which includes Becke–Johnson damping [67]. Additionally, corrections for reactions in the liquid phase were made using the SMD polarizable continuum solvent model [68], augmented with parameters for toluene.

4. Conclusions

The selective nature of Cr-PNP catalysts for the tri- and tetramerizations of ethylene is of immense interest to experimental and theoretical chemists. However, theoretical studies on Cr-PNP catalysts are scarce in the literature. We carried out a DFT study using the real Sasol catalyst following the metallacycle mechanism, which has already been established by many experimental and theoretical studies. In this DFT study, we considered the oxidation state of Cr as I/III. The Gibbs free energy profile at 298.15K for the full potential energy surfaces of the *ortho*- and *para*-methoxyaryl Cr-PNP catalysts indicates that the trimerization of ethylene is kinetically feasible in both cases. However, the ligand backbone seems to play a vital role towards the selectivity. The propensity for trimerization is caused by the hemilabile *ortho*-methoxy group with steric hindrance. The swing from the tri- to tetramerization of ethylene with the *para*-methoxyaryl Cr-PNP ligand seems to be caused by moving the *ortho*-methoxy group out of the coordination sphere.

Supplementary Materials: The following supporting information can be downloaded at: <https://www.mdpi.com/article/10.3390/molecules28073101/s1>. Optimized coordinates of the DFT calculations.

Author Contributions: Conceptualization, M.C.; methodology, M.C.; software, M.C.; validation, M.C.; formal analysis, M.C.; investigation, M.C.; resources, M.C.; data curation, M.C.; writing—original draft preparation, M.C. and A.S.; writing—review and editing, M.C.; visualization, M.C.; supervision, M.C.; project administration, M.C.; funding acquisition, M.C. All authors have read and agreed to the published version of the manuscript.

Funding: This research was funded by KIST Institutional Program (Atmospheric Environment Research Program, Project No. 2E31690).

Institutional Review Board Statement: Not applicable.

Informed Consent Statement: Not applicable.

Data Availability Statement: Data are available within the article and the Supplementary Materials.

Conflicts of Interest: The authors declare no conflict of interest. The funders had no role in the design of the study; in the collection, analyses, or interpretation of data; in the writing of the manuscript; or in the decision to publish the results.

References

1. Skupinska, J. Oligomerization of α -olefins to higher oligomers. *Chem. Rev.* **1991**, *91*, 613–648. [[CrossRef](#)]
2. Keim, W.; Kowaldt, F.H.; Goddard, R.; Krüger, C. Novel coordination of (benzoylmethylene)triphenylphosphorane in a nickel oligomerization catalyst. *Angew. Chem. Int. Ed. Engl.* **1978**, *17*, 466–467. [[CrossRef](#)]
3. Svejda, S.A.; Brookhart, M. Ethylene oligomerization and propylene dimerization using cationic (α -diimine)nickel(II) catalysts. *Organometallics* **1999**, *18*, 65–74. [[CrossRef](#)]
4. Killian, C.M.; Johnson, L.K.; Brookhart, M. Preparation of linear α -olefins using cationic nickel(II) α -diimine catalysts. *Organometallics* **1997**, *16*, 2005–2007. [[CrossRef](#)]
5. Mecking, S. Cationic nickel and palladium complexes with bidentate ligands for the C-C linkage of olefins. *Coord. Chem. Rev.* **2000**, *203*, 325–351. [[CrossRef](#)]
6. Ruther, T.; Braussaud, N.; Cavell, K.J. Novel chromium(III) complexes containing imidazole-based chelate ligands with varying donor sets: synthesis and reactivity. *Organometallics* **2001**, *20*, 1247–1250. [[CrossRef](#)]
7. Britovsek, G.J.P.; Mastroianni, S.; Solan, G.A.; Baugh, S.P.D.; Redshaw, C.; Gibson, V.C.; White, A.J.P.; Williams, D.J.; Elsegood, M.R.J. Oligomerization of ethylene by bis(imino)pyridyliron and -cobalt complexes. *Chem. Eur. J.* **2000**, *6*, 2221–2231. [[CrossRef](#)] [[PubMed](#)]
8. Vogt, D. Oligomerization of ethylene to higher linear α -olefins. In *Applied Homogeneous Catalysis with Organometallic Compounds*; Cornils, B., Herrmann, W.A., Eds.; VCH: Weinheim, Germany, 2000; pp. 245–258.
9. Reagan, W.K. Phillips Petroleum Company. EU Patent 0417477, 20 March 1991.
10. McGuinness, D.S.; Brown, D.B.; Tooze, D.B.; Hess, F.M.; Dixon, J.T.; Slawin, A.M.Z. Ethylene trimerization with Cr-PNP and Cr-SNS complexes: Effect of ligand structure, metal oxidation state, and role of activator on catalysis. *Organometallics* **2006**, *25*, 3605–3610. [[CrossRef](#)]
11. Bollmann, A.; Blann, K.; Dixon, J.T.; Hess, F.M.; Killan, E.; Maumela, H.; McGuinness, D.; Morgan, D.H.; Neveling, A.; Otto, S.; et al. Ethylene tetramerization: A new route to produce 1-octene in exceptionally high selectivities. *J. Am. Chem. Soc.* **2004**, *126*, 14712–14713. [[CrossRef](#)] [[PubMed](#)]
12. Kim, S.-K.; Kim, T.-J.; Chung, J.-H.; Hahn, T.-K.; Chae, S.-S.; Lee, H.-S.; Cheong, M.; Kang, S.O. Bimetallic ethylene tetramerization catalysts derived from chiral DPPDME ligands: Syntheses, structural characterizations, and catalytic performance of [(DPPDME)CrCl₃]₂ (DPPDME = S,S- and R,R-chiraphos and meso-achiraphos). *Organometallics* **2010**, *29*, 5805–5811. [[CrossRef](#)]
13. Son, K.; Waymouth, R.M. Selective ethylene oligomerization in the presence of ZnR₂: Synthesis of terminally-functionalized ethylene oligomers. *Organometallics* **2010**, *29*, 3515–3520. [[CrossRef](#)]
14. Manyik, R.M.; Walker, W.E.; Wilson, T.P. Union Carbide Corporation. U.S. Patent 3300458, 1967.
15. Briggs, J.R. The selective trimerization of ethylene to hex-1-ene. *Chem. Commun.* **1989**, *11*, 674–675. [[CrossRef](#)]
16. Emrich, R.; Heinemann, O.; Jolly, P.W.; Krueger, C.; Verhovnik, G.P.J. The role of metallacycles in the chromium-catalyzed trimerization of ethylene. *Organometallics* **1997**, *16*, 1511–1513. [[CrossRef](#)]
17. Cossee, P. Ziegler-Natta catalysis I. Mechanism of polymerization of α -olefins with Ziegler-Natta catalysts. *J. Catal.* **1964**, *3*, 80–88. [[CrossRef](#)]
18. Arlman, E.J.; Cossee, P. Ziegler-Natta catalysis III. Stereospecific polymerization of propene with the catalyst system TiCl₃-AlEt₃. *J. Catal.* **1964**, *3*, 99–104. [[CrossRef](#)]

19. Agapie, T.; Schofer, S.J.; Labinger, J.A.; Bercaw, J.E. Mechanistic studies of the ethylene trimerization reaction with chromium-diphosphine catalysts: Experimental evidence for a mechanism involving metallacyclic intermediates. *J. Am. Chem. Soc.* **2004**, *126*, 1304–1305. [[CrossRef](#)]
20. Agapie, T.; Labinger, J.A.; Bercaw, J.E. Mechanistic studies of olefin and alkyne trimerization with chromium catalysts: Deuterium labeling and studies of regiochemistry using a model chromacyclopentane complex. *J. Am. Chem. Soc.* **2007**, *129*, 14281–14295. [[CrossRef](#)]
21. Arteaga-Müller, R.; Tsurugi, H.; Saito, T.; Yanagawa, M.; Oda, S.; Mashima, K. New Tantalum ligand-free catalyst system for highly selective trimerization of ethylene affording 1-hexene: New evidence of a metallacycle mechanism. *J. Am. Chem. Soc.* **2009**, *131*, 5370–5371. [[CrossRef](#)]
22. Wass, D.F. Chromium-catalysed ethene trimerisation—Breaking the rules in olefin oligomerisation. *Dalton Trans.* **2007**, *2007*, 816–819. [[CrossRef](#)]
23. Dixon, J.T.; Green, M.J.; Hess, F.M.; Morgan, D.H. Advances in selective ethylene trimerisation—A critical overview. *J. Organomet. Chem.* **2004**, *689*, 3641–3668. [[CrossRef](#)]
24. Fang, Y.; Liu, Y.; Ke, Y.; Guo, C.; Zhu, N.; Mi, X.; Ma, Z.; Hu, Y. A new chromium-based catalyst coated with paraffin for ethylene oligomerization and the effect of chromium state on oligomerization selectivity. *Appl. Catal. A* **2002**, *235*, 33–38. [[CrossRef](#)]
25. Ban, K.; Hayashi, T.; Suzuki, Y. Mitsui Chemicals Incorporated. JP Patent 11060627, 2 March 1999.
26. Cotton, F.A.; Wilkinson, G.; Murillo, C.A.; Bochmann, M. *Advanced Inorganic Chemistry*; John Wiley and Sons, Inc.: New York, NY, USA, 1999; p. 1355.
27. Poli, R. Open shell organometallics: A general analysis of their electronic structure and reactivity. *J. Organomet. Chem.* **2004**, *689*, 4291–4304. [[CrossRef](#)]
28. Poli, R.; Harvey, J.N. Spin forbidden chemical reactions of transition metal compounds. New ideas and new computational challenges. *Chem. Soc. Rev.* **2003**, *32*, 1–8. [[CrossRef](#)] [[PubMed](#)]
29. Green, J.C.; Harvey, J.N.; Poli, R. Theoretical investigation of the spin crossover transition states of the addition of methane to a series of Group 6 metallocenes using minimum energy crossing points. *J. Chem. Soc. Dalton Trans.* **2002**, *8*, 1861–1866. [[CrossRef](#)]
30. Harvey, J.N.; Aschi, M.; Schwarz, H.; Koch, W. The singlet and triplet states of phenyl cation. A hybrid approach for locating minimum energy crossing points between non-interacting potential energy surfaces. *Theor. Chem. Acc.* **1998**, *99*, 95–99. [[CrossRef](#)]
31. Hossain, M.A.; Kim, H.S.; Houk, K.N.; Cheong, M. Spin-crossover in chromium-catalyzed ethylene trimerization: Density functional theory study. *Bull. Korean Chem. Soc.* **2014**, *35*, 2835–2838. [[CrossRef](#)]
32. Budzelaar, P.H.M. Ethene trimerization at Cr^I/Cr^{III}—A density functional theory (DFT) study. *Can. J. Chem.* **2009**, *87*, 832–837. [[CrossRef](#)]
33. Britovsek, G.J.P.; McGuinness, D.S.; Wierenga, T.S.; Young, C.T. Single- and double-coordination mechanism in ethylene tri- and tetramerization with Cr/PNP catalysts. *ACS Catal.* **2015**, *5*, 4152–4166. [[CrossRef](#)]
34. Gong, M.; Liu, Z.; Li, Y.; Ma, Y.; Sun, Q.; Zhang, J.; Liu, B. Selective co-oligomerization of ethylene and 1-hexene by chromium-PNP catalysts: A DFT study. *Organometallics* **2016**, *35*, 972–981. [[CrossRef](#)]
35. Köhn, R.D. Reactivity of chromium complexes under spin control. *Angew. Chem. Int. Ed.* **2008**, *47*, 245–247. [[CrossRef](#)]
36. Schofer, S.J.; Day, M.W.; Henling, L.M.; Labinger, J.A.; Bercaw, J.E. Ethylene trimerization catalysts based on chromium complexes with a nitrogen-bridged diphosphine ligand having *ortho*-methoxyaryl or *ortho*-thiomethoxy substituents: Well-defined catalyst precursors and investigations of the mechanism. *Organometallics* **2006**, *25*, 2743–2749. [[CrossRef](#)]
37. Manyik, R.M.; Walker, W.E.; Wilson, T.P. A soluble chromium-based catalyst for ethylene trimerization and polymerization. *J. Catal.* **1977**, *47*, 197–209. [[CrossRef](#)]
38. Yang, Y.; Kim, H.; Lee, J.; Paik, H.; Jang, H.G. Roles of chloro compound in homogeneous [Cr(2-ethylhexanoate)₃/2,5-dimethylpyrrole/triethylaluminum/chloro compound] catalyst system for ethylene trimerization. *Appl. Catal. A* **2000**, *193*, 29–38. [[CrossRef](#)]
39. Wasserscheid, P.; Grimm, S.; Köhn, R.D.; Haufe, M. Synthesis of synthetic lubricants by trimerization of 1-decene and 1-dodecene with homogeneous chromium catalysts. *Adv. Synth. Catal.* **2001**, *343*, 814. [[CrossRef](#)]
40. Carter, A.; Cohen, S.A.; Cooley, N.A.; Murphy, A.; Scutt, J.; Wass, D.F. High activity ethylene trimerisation catalysts based on diphosphine ligands. *J. Chem. Soc. Chem. Commun.* **2002**, *8*, 858–859. [[CrossRef](#)]
41. Monoi, T.; Sasaki, Y. Silica-supported Cr[N(SiMe₃)₂]₃/isobutylalumoxane catalyst for selective ethylene trimerization. *J. Mol. Catal. A Chem.* **2002**, *187*, 135–141. [[CrossRef](#)]
42. McGuinness, D.S.; Wasserscheid, P.; Keim, W.; Hu, C.; Englert, U.; Dixon, J.T.; Grove, C. Novel Cr-PNP complexes as catalysts for the trimerisation of ethylene. *J. Chem. Soc. Chem. Commun.* **2003**, *2003*, 334–335. [[CrossRef](#)]
43. McGuinness, D.S.; Wasserscheid, P.; Keim, W.; Morgan, D.; Dixon, J.T.; Bollmann, A.; Maumela, H.; Hess, F.; Englert, U. First Cr(III)-SNS complexes and their use as highly efficient catalysts for the trimerization of ethylene to 1-hexene. *J. Am. Chem. Soc.* **2003**, *125*, 5272–5273. [[CrossRef](#)]
44. Morgan, D.H.; Schwikkard, S.L.; Dixon, J.T.; Nair, J.J.; Hunter, R. The effect of aromatic ethers on the trimerisation of ethylene using a chromium catalyst and aryloxy ligands. *Adv. Synth. Catal.* **2003**, *345*, 939–942. [[CrossRef](#)]
45. Commereuc, D.; Drochon, S.; Saussine, L. Institut Francais du Petrole. U.S. Patent 6031145, 2000.
46. Wu, F.-J. Amoco Corp. U.S. Patent 5811618, 1998.
47. Aoyama, T.; Mimura, H.; Yamamoto, T.; Oguri, M.; Koie, Y. Tosoh Corp. JP Patent 09176229, 1997.

48. Jolly, P.W. From hein to hexene: Recent advances in the chemistry of organochromium π -complexes. *Acc. Chem. Res.* **1996**, *29*, 544–551. [[CrossRef](#)]
49. Deckers, P.J.W.; Hessen, B.; Teuben, J.H. Switching a catalyst System from ethene polymerization to ethene trimerization with a hemilabile ancillary ligand. *Angew. Chem. Int. Ed.* **2001**, *40*, 2516–2519. [[CrossRef](#)]
50. Deckers, P.J.W.; Hessen, B.; Teuben, J.H. Catalytic trimerization of ethene with highly active cyclopentadienyl-arene titanium catalysts. *Organometallics* **2002**, *21*, 5122–5135. [[CrossRef](#)]
51. Pellecchia, C.; Pappalardo, D.; Oliva, L.; Mazzeo, M.; Gruter, G.-J. Selective co-oligomerization of ethylene and styrenes by half-titanocene catalysts and synthesis of polyethylenes with 4-aryl-1-butyl branches. *Macromolecules* **2000**, *33*, 2807–2814. [[CrossRef](#)]
52. Andes, C.; Harkins, S.B.; Murtuza, S.; Oyler, K.; Sen, A. New tantalum-based catalyst system for the selective trimerization of ethene to 1-hexene. *J. Am. Chem. Soc.* **2001**, *123*, 7423–7424. [[CrossRef](#)]
53. Santi, R.; Romano, A.M.; Grande, M.; Sommazzi, A.; Masi, F.; Proto, A. ENICHEM S.P.A. WO 0168572. 2001.
54. Overett, M.J.; Blann, K.; Bollmann, A.; Dixon, J.T.; Hess, F.; Killian, E.; Maumela, H.; Morgan, D.H.; Neveling, A.; Otto, S. Ethylene trimerisation and tetramerisation catalysts with polar-substituted diphosphinoamine ligands. *J. Chem. Soc. Chem. Commun.* **2005**, *5*, 622–624. [[CrossRef](#)]
55. Bhaduri, S.; Mukhopadhyay, S.; Kulkarni, S.A. Density functional studies on chromium catalyzed ethylene trimerization. *J. Organomet. Chem.* **2009**, *694*, 1297–1307. [[CrossRef](#)]
56. de Bruin, T.J.M.; Magna, L.; Raybaud, P.; Toulhoat, H. Hemilabile ligand induced selectivity: A DFT study on ethylene trimerization catalyzed by titanium complexes. *Organometallics* **2003**, *22*, 3404–3413. [[CrossRef](#)]
57. Overett, M.J.; Blann, K.; Bollmann, A.; Dixon, J.T.; Haasbroek, D.; Killian, E.; Maumela, H.; McGuinness, D.S.; Morgan, D.H. Mechanistic investigations of the ethylene tetramerisation reaction. *J. Am. Chem. Soc.* **2005**, *127*, 10723–10730. [[CrossRef](#)]
58. Brookhart, M.; Green, M.L.H.; Parkin, G. Agostic interactions in transition metal compounds. *Proc. Natl. Acad. Sci. USA* **2007**, *104*, 6908–6914. [[CrossRef](#)]
59. Yu, Z.-X.; Houk, K.N. Why trimerization? Computational elucidation of the origin of selective trimerization of ethene catalyzed by $[\text{TaCl}_3(\text{CH}_3)_2]$ and an agostic-assisted hydride transfer mechanism. *Angew. Chem. Int. Ed.* **2003**, *42*, 808–811. [[CrossRef](#)] [[PubMed](#)]
60. Becke, A.D. Density-functional exchange-energy approximation with correct asymptotic behavior. *Phys. Rev. A* **1988**, *38*, 3098–3100. [[CrossRef](#)] [[PubMed](#)]
61. Lee, C.; Yang, W.; Parr, R.G. Development of the Colle-Salvetti correlation-energy formula into a functional of the electron density. *Phys. Rev. B* **1988**, *37*, 785–789. [[CrossRef](#)]
62. Becke, A.D. Density-functional thermochemistry. III. The role of exact exchange. *J. Chem. Phys.* **1993**, *98*, 5648–5652. [[CrossRef](#)]
63. Check, C.E.; Faust, T.O.; Bailey, J.M.; Wright, B.J.; Gilbert, T.M.; Sunderlin, L.S. Addition of polarization and diffuse functions to the LANL2DZ basis set for p-block elements. *J. Phys. Chem. A* **2001**, *105*, 8111–8116. [[CrossRef](#)]
64. Dines, T.J.; Inglis, S. Raman spectroscopic study of supported chromium(vi) oxide catalysts. *Phys. Chem. Chem. Phys.* **2003**, *5*, 1320–1328. [[CrossRef](#)]
65. Frisch, M.J.; Trucks, G.W.; Schlegel, H.B.; Scuseria, G.E.; Robb, M.A.; Cheeseman, J.R.; Scalmani, G.; Barone, V.; Petersson, G.A.; Nakatsuji, H.; et al. *Gaussian 16*; Gaussian, Inc.: Wallingford, CT, USA, 2016.
66. Grimme, S.; Antony, J.; Ehrlich, S.; Krieg, H. A consistent and accurate ab initio parametrization of density functional dispersion correction (DFT-D) for the 94 elements H–Pu. *J. Chem. Phys.* **2010**, *132*, 154104. [[CrossRef](#)]
67. Grimme, S.; Ehrlich, S.; Goerigk, L. Effect of the damping function in dispersion corrected density functional theory. *J. Comput. Chem.* **2011**, *32*, 1457–1465. [[CrossRef](#)]
68. Marenich, A.V.; Cramer, C.J.; Truhlar, D.G. Universal solvation model based on solute electron density and on a continuum model of the solvent defined by the bulk dielectric constant and atomic surface tensions. *J. Phys. Chem. B* **2009**, *113*, 6378–6396. [[CrossRef](#)] [[PubMed](#)]

Disclaimer/Publisher's Note: The statements, opinions and data contained in all publications are solely those of the individual author(s) and contributor(s) and not of MDPI and/or the editor(s). MDPI and/or the editor(s) disclaim responsibility for any injury to people or property resulting from any ideas, methods, instructions or products referred to in the content.